

Synthesis of Pt–Sn nanoalloy catalysts with enhanced performance in the dehydrogenation of propane

Zhanhua Ma¹, Aijing Jiang¹, Shuai Li¹, Jun Li¹, Lanyi Sun¹, Changhua An² ✉

¹State Key Laboratory of Heavy Oil Processing, College of Chemical Engineering, China University of Petroleum (East China), Shandong, Qingdao 266580, People's Republic of China

²Tianjin Key Laboratory of Organic Solar Cells and Photochemical Conversion College of Chemistry and Chemical Engineering, School of Chemistry and Chemical Engineering, Tianjin University of Technology, Tianjin 300384, People's Republic of China

✉ E-mail: anch@tjut.edu.cn

Published in *Micro & Nano Letters*; Received on 4th April 2018; Revised on 10th February 2019; Accepted on 27th February 2019

Platinum–tin (Pt–Sn) nanoalloy catalyst supported on Al₂O₃ was prepared by carbonylation–impregnation method. The catalyst was characterised by means of nitrogen adsorption–desorption, X-ray diffraction and transmission electron microscope, showing the existence of Pt and Sn as Pt₃Sn alloy. The analysis of particle size distribution revealed that Pt–Sn nanoparticles have high dispersion and narrow particle size distribution with an average diameter of 1.7 ± 0.4 nm. Its catalytic performance toward propane dehydrogenation was also investigated. The propane dehydrogenation reaction showed that the as-prepared Pt–Sn/Al₂O₃ catalyst exhibited good dehydrogenation performance with the conversion of 27.1% and propylene selectivity of 93.3% after reacting 12 h owing to the close interaction between Pt and Sn components. Coke deposition of the used catalyst was characterised by thermogravimetric and differential thermal analysis method, revealing most of the carbon was on the surface of the support, which meant that more active sites to be accessible to maintain catalytic stability.

1. Introduction: Propylene is an important chemical raw material and intermediate. With the increasing demand for propylene derivatives such as polypropylene, acrylic acid, acrylonitrile and epoxypropane, the demand for propylene has also increased quickly [1–4]. As petroleum gas and shale gas contain a large amount of propane, the process of propane dehydrogenation has become the third important source of propylene in recent years [5, 6].

As an important commercial technology in propane dehydrogenation, Oleflex technology of universal oil products (UOP) adopts platinum (Pt)-based catalyst, of which Al₂O₃ is used as a support with Pt as an active component and elements of tin (Sn), Ir and K as promoters [5, 7]. Since propane dehydrogenation is an endothermic reaction, the reaction temperature is normally above 550°C to achieve a considerable conversion. However, for Pt/Al₂O₃, the high temperature will quickly deactivate the catalyst due to the sintering of Pt and carbon deposit [8]. Introducing additive Sn can improve the dehydrogenation performance of Pt-based catalyst. On one hand, Sn can divide the large Pt atom clusters on support surface into smaller ones, inhibiting the multi-point adsorption of hydrocarbon molecules on the Pt surface and reducing hydrogenolysis and carbon deposit [9]. On the other hand, the electron from Sn²⁺ (or metallic Sn) can be transferred to Pt_{5d} orbital, decreasing the interaction between Pt and hydrocarbon, which is beneficial for the propylene stripping, reducing deep dehydrogenation and decomposition of olefin [10].

Despite extensive research has been made, the state of Sn in Pt–Sn catalyst is still under debate. Some researchers contend that Sn existed on the catalyst as oxidic and chloridic Sn²⁺/Sn⁴⁺ species [5]. However, other researchers demonstrated that Sn and Pt catalysts exist in the form of Pt–Sn alloy [11–13]. Kappenstein *et al.* [11] prepared Pt–Sn/Al₂O₃ catalyst and found that most Sn was reduced into Sn⁰ in the form of PtSn and Pt₃Sn alloys. Vu *et al.* [12] studied Pt–Sn/Al₂O₃ and Pt–Sn/ZnAl₂O₄ and found that the Sn of reduced Pt–Sn/Al₂O₃ existed mainly in the form of PtSn and Pt₃Sn. Yang *et al.* [13] simulated the propane dehydrogenation activities on the surfaces of three alloys

(Pt₃Sn, Pt₂Sn and PtSn₂) as well as the propylene selectivity based on density functional theory. They found that the propylene stripping on the surface of Pt–Sn alloy is favoured in dynamics. By comparing catalytic activity and selectivity among three alloys, Pt₃Sn had the optimal propane dehydrogenation property. However, the Pt–Sn/Al₂O₃ catalysts are generally prepared by using conventional impregnation method. Sn was introduced both into the surface of Pt particles and support, and the alloy type cannot be controlled, which led to the partial formation of Pt–Sn alloys paralleling the metal Pt⁰. The low concentration of Pt–Sn alloys may be one of the causes for the low selectivity owing to destructive hydrogenolysis [14]. The carbonyl synthesis route is one of the ways to generate definite bimetallic catalysts, of which Pt and Sn are in the same particle [15]. In this Letter, the Pt–Sn carbonyl clusters were first synthesised by a carbonylation reaction before impregnation in order to precisely control the Sn deposition at the atomic level and increase the concentration of Pt–Sn alloys and corresponding catalytic performance.

2. Experimental procedure: Pt–Sn/Al₂O₃ catalyst (with Pt loading of 0.5 wt%) was prepared by carbonylation–impregnation method as follows: (i) certain amount of Na₂PtCl₆·6H₂O, SnCl₄·5H₂O and CH₃COONa·3H₂O were dissolved in methyl alcohol, with CH₃COONa/Pt molar ratio of 8:1 and Pt–Sn molar ratio of 3:1. The carbonylation reaction was performed at 50°C in the atmosphere of CO, resulting in the formation of green Pt–Sn carbonyl compound. (ii) Al₂O₃ was added for loading 12 h. The catalyst can be obtained by decarbonylation at 200°C in the atmosphere of N₂ for 1 h, denoted as Pt₃Sn/Al₂O₃. For comparison, non-supported Pt–Sn alloy sample was prepared with a similar procedure, denoted as Pt₃Sn. Pt–Sn/Al₂O₃ catalyst was also prepared by the incipient-wetness impregnation method with Pt loading of 0.5 wt% and Pt–Sn molar ratio of 3:1, assigned as Pt–Sn_(im)/Al₂O₃.

The physical structure of the prepared catalyst was characterised by N₂ absorption–desorption (Micromeritics Instrument Corporation, ASAP3020). The phase analysis of catalyst was

performed by X-ray diffraction (XRD) (PANalytical Co., Netherlands, Model X'Pert Pro MPD), using Cu-K α ray as a light source, at a scan rate of 7°/min and scan range from 5° to 75°. The grain size of Pt–Sn nanoparticles and surface topography of catalyst were measured using transmission electron microscope (TEM) (FEI Co., Model Tecnai G2F20) at a point resolution of 0.248 nm, line resolution of 0.102 nm and an accelerating voltage of 200 kV. The samples were prepared by ultrasonically suspending the catalyst powder in alcohol, and a drop of the solution was placed onto a carbon film-coated Cu grid. The carbon deposit was investigated by thermogravimetric and differential thermal analysis (TG-DTA) on model WCT-2 thermo-balance apparatus (Beijing Optical Instrument Factory). An ~10.0 mg catalyst was heated from room temperature to 800°C at a rate of 10°C/min in flowing air.

The propane dehydrogenation property of prepared catalyst was evaluated at atmospheric pressure in an MRCS-8007 continuous fixed-bed tubular reactor. The filling weight of catalyst was 1.0 g and the reaction temperature was set to 580°C. Prior to reaction, the temperature was increased from room temperature to 580°C in the atmosphere of H₂, with an increasing rate of 5°C/min. The gases' flow rate was 44 ml/min with H₂/C₃H₈ molar ratio of 1:4 and weight hourly space velocity (WHSV) of 4.0 h⁻¹. Online analysis of the resulting product was conducted using an SP-2100 gas chromatograph. Propane conversion, propylene selectivity and yield were calculated by normalisation method of a carbon atom. The carbon balance calculated was 95 ± 5%. The turnover frequency (TOF) (s⁻¹) of C₃H₆ is shown in the equation below:

$$\text{TOF} = \frac{n_{\text{C}_3}^{\text{inlet}} \times \text{conv.} \times \text{selec.} \times 195.08}{m_{\text{cat}} \times w_{\text{Pt}}} \quad (1)$$

In which, $n_{\text{C}_3}^{\text{inlet}}$ is the flow rate of propane in the feed, mol/s; conv. is the conversion of propane; selec. is the selectivity of propylene; 195.08 is the atomic weight of Pt, g/mol; m_{cat} is the weight of the catalyst, g; and w_{Pt} is a mass fraction of Pt on the catalyst.

3. Results and discussion: The N₂ adsorption and desorption isotherms of Al₂O₃ and Pt₃Sn/Al₂O₃ were given in Fig. 1. From Fig. 1a, a typical type-IV isotherm with H1 hysteresis loop for Al₂O₃ support indicates its mesoporous channel. This characteristic is confirmed by the pore size distribution of Al₂O₃ in Fig. 1b. The calculation by the Barrett–Joyner–Halenda (BJH) method shows the pore sizes of the support are mainly within 5–8 nm. Pt₃Sn/Al₂O₃ sample has a similar feature to Al₂O₃ support, except the peak intensity is decreased. After loading active components, the Brunauer–Emmett–Teller (BET) of Al₂O₃ is decreased from 239.5 to 204.3 m²/g, the mean pore size is decreased from 7.02 to 6.23 nm and the pore volume is reduced from 0.53 to 0.45 cm³/g. This is mainly due to that the active components blocked some porous channels.

Fig. 2 shows XRD patterns of Pt₃Sn, Pt₃Sn/Al₂O₃ (Pt loading amount of 10 wt%) and Al₂O₃ samples. The diffraction peaks located at 31.5°, 38.7°, 45.1° and 65.7° can be indexed to the facets of (110), (111), (200) and (220) of Pt₃Sn alloy [9–11]. Obviously, the locations are the same as the non-supported Pt₃Sn sample. For Pt₃Sn/Al₂O₃ sample, these peaks overlap with the peaks of alumina support, indicating the high metal dispersion on the support. Compared to Al₂O₃ support, the intensity of typical Pt₃Sn (111) crystal face peak shows an increase for Pt₃Sn/Al₂O₃ sample, pointing out the possibility of the existence of Pt₃Sn alloy on the catalyst. The theoretical calculation [13] shows that crystal face (111) of Pt₃Sn has a relatively weaker adsorption capacity for propane, and thus decreases the occurrence of deep dehydrogenation of propane and other side reactions.

Fig. 3 shows TEM characterisation of Pt₃Sn/Al₂O₃ sample. According to Fig. 3a, it can be seen the Pt–Sn particles are substantially uniformly distributed and have a narrow particle size

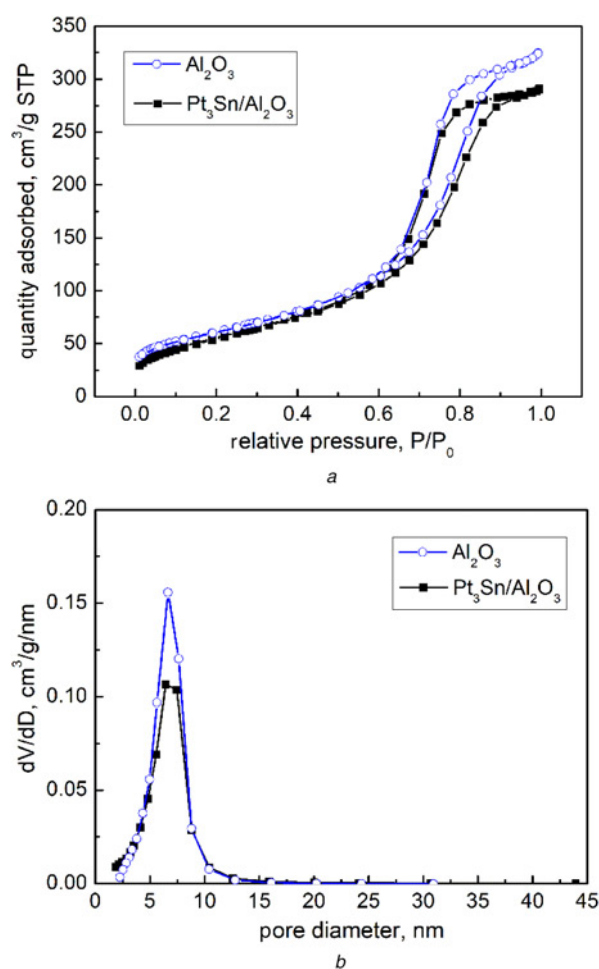


Fig. 1 N₂ adsorption–desorption isotherms and pore size distributions of Al₂O₃ and Pt₃Sn/Al₂O₃ sample
a N₂ adsorption–desorption isotherms
b Pore size distribution

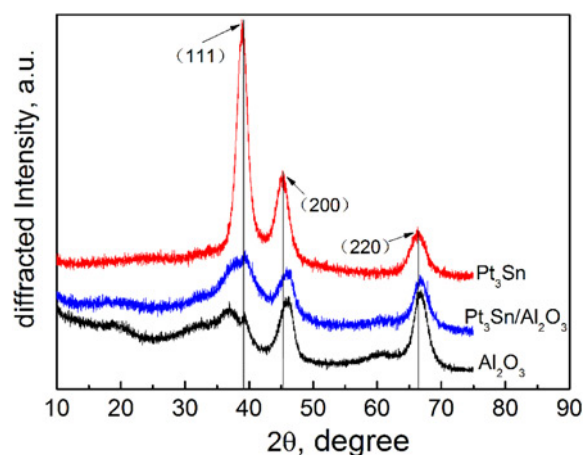


Fig. 2 XRD patterns of Pt₃Sn, Pt₃Sn/Al₂O₃ and Al₂O₃

distribution, ranging from 0.9 to 3.1 nm with a mean diameter of 1.7 ± 0.4 nm. Fig. 3b shows the high-resolution TEM (HRTEM) image of Pt₃Sn/Al₂O₃ sample, indicating the presence of Pt–Sn crystallite with clear lattice fringes. Fast Fourier transform (FFT) was applied to calculate the lattice spacing. The FFT image inset of Fig. 3b exhibits the lattice spacings of 0.23 and 0.20 nm that match the (111) and (200) reflection planes of the Pt₃Sn alloy, respectively. The carbonyl pathway adopted in this work

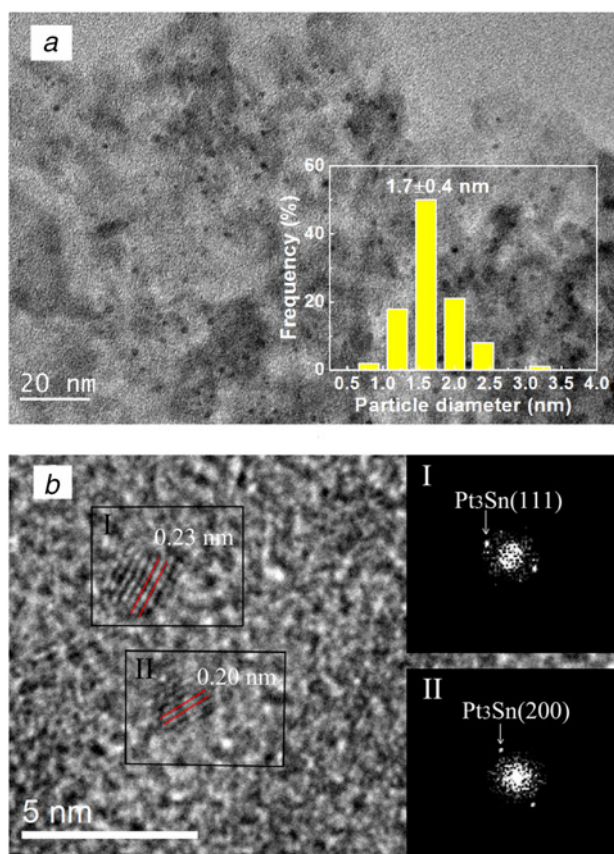


Fig. 3 TEM, size distribution and HRTEM images of $\text{Pt}_3\text{Sn}/\text{Al}_2\text{O}_3$ sample
 a TEM image and size distribution (inset)
 b HRTEM image

may allow the synthesis of bimetallic Pt_xSn_y carbonyl cluster (Pt-Sn-CO). The results of Shitova *et al.* [16] showed that the Pt-Sn-CO cluster could strongly adsorb on Al_2O_3 support and did not change its composition. This made the preparation of supported catalysts with definite compositions possible. Moreover, this method can help to bind Pt metal particles to the oxygen atoms of Al_2O_3 support and increase the dispersion attributing to the oxophilic character of Sn [17].

Fig. 4 reveals the propane dehydrogenation performance of $\text{Pt}_3\text{Sn}/\text{Al}_2\text{O}_3$ and $\text{Pt-Sn}_{(\text{im})}/\text{Al}_2\text{O}_3$. It can be seen from Fig. 4a that the initial propane conversion is 31.5%, selectivity is 88.0% and propylene yield is 27.7% for the $\text{Pt}_3\text{Sn}/\text{Al}_2\text{O}_3$ catalyst. With the extension of reaction time in the early stage, the propane conversion is slightly reduced, and propylene selectivity is increased. After reacting 0.75 h, the propane conversion decreases from 31.5 to 29.2%, with the selectivity increasing from 88.0 to 94.3% and the propylene yield of 28.0%. With the further extension of reaction, the catalyst activity remains unchanged after 2.5 h, showing high stability. Meanwhile, the TOF of propylene formation reaches the maximum value of 0.29 s^{-1} at 0.75 h and then shows a similar trend as propane conversion and propylene yield, and finally remains stable at 0.27 s^{-1} after reacting 2.5 h. Fig. 4b shows the $\text{Pt-Sn}_{(\text{im})}/\text{Al}_2\text{O}_3$ catalyst exhibits low propylene selectivity. With prolonging the reaction, the propane conversion reduces and propylene selectivity increases, while the propylene yield and TOF of propylene formation increase gradually. After 12 h, the propylene yield of 18.8% and TOF of 0.19 s^{-1} is attained. On the basis of the results, it can be concluded that the catalytic performance of $\text{Pt}_3\text{Sn}/\text{Al}_2\text{O}_3$ catalyst is better than that of $\text{Pt-Sn}_{(\text{im})}/\text{Al}_2\text{O}_3$ catalyst. Particularly, both the propylene selectivity and TOF of the former are higher than those of the latter. The

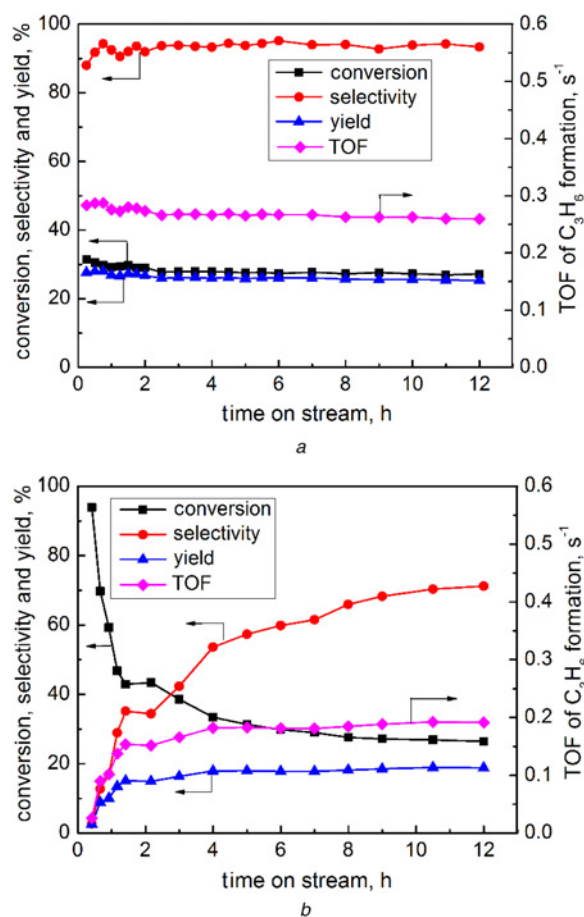


Fig. 4 Propane conversion, propylene selectivity, propylene yield and TOF versus time
 a $\text{Pt}_3\text{Sn}/\text{Al}_2\text{O}_3$ catalyst
 b $\text{Pt-Sn}_{(\text{im})}/\text{Al}_2\text{O}_3$ catalyst

Table 1 Comparisons of evaluation conditions and catalytic performance of Pt- or Pt-Sn-based catalysts

Sample	$T, ^\circ\text{C}$	Time, h	WHSV, h^{-1}	Conv.	Selec.	TOF, s^{-1}
$\text{Pt}/\text{Al}_2\text{O}_3$	600	0	3.8	0.32	0.85	0.42
[18]	—	14	3.8	0.17	0.86	0.23
$\text{Pt-Sn}/\text{Al}_2\text{O}_3$	590	0	3.0	0.29	0.80	0.17
[19]	—	6	3.0	0.23	0.93	0.16
$\text{Pt-Sn}/1.5\text{In}$	580	0	0.56	0.39	0.98	0.09
$-\text{Al}_2\text{O}_3$ [20]	—	—	—	—	—	—
$\text{Pt-Sn}/\text{SUZ}$	590	0	3.0	0.25	0.84	0.15
-4 [21]	—	10	3.0	0.22	0.93	0.14

formation of Pt_3Sn alloy has a significant promotion effect on the catalytic performance in propane dehydrogenation for $\text{Pt-Sn}/\text{Al}_2\text{O}_3$ catalyst.

Table 1 summarises the evaluation conditions for Pt- and Pt-Sn-based catalysts in propane dehydrogenation as well as corresponding TOF data in recent years. It indicates that $\text{Pt}_3\text{Sn}/\text{Al}_2\text{O}_3$ catalyst in this work has better dehydrogenation performance, and the TOF of propylene formation over $\text{Pt}_3\text{Sn}/\text{Al}_2\text{O}_3$ is higher than that over some reported Pt-Sn-based catalysts, but lower than that over Pt-based catalyst. Nevertheless, Pt-based catalyst has poor stability, of which the TOF was decreased from 0.42 to 0.23 s^{-1} after the reaction continued for 14 h. Therefore, the as-prepared $\text{Pt}_3\text{Sn}/\text{Al}_2\text{O}_3$ catalyst has better dehydrogenation performance. This result could be attributed to the close interaction between Pt and

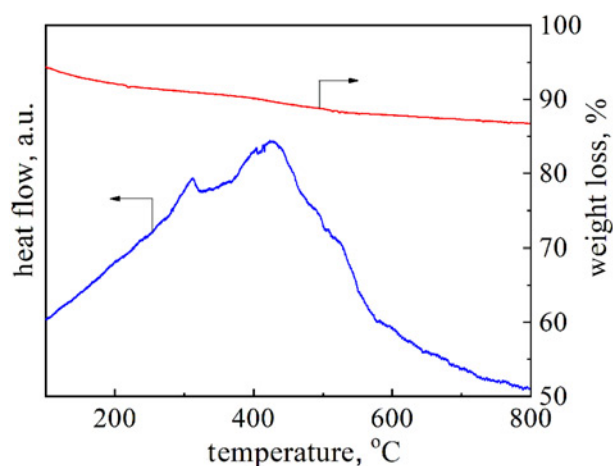


Fig. 5 TG-DTA profiles of the catalysts after reaction at 580°C for 12 h

Sn components due to the directly adopting Pt_3Sn_y carbonyl cluster as a precursor, leading to a desired active centre and avoiding the waste of Sn promoter.

Fig. 5 shows the TG-DTA curves of $\text{Pt}_3\text{Sn}/\text{Al}_2\text{O}_3$ catalyst after reaction of 12 h. There are three exothermic peaks on the catalyst, each of which represents a particular type of coke deposit [22–24]. The exothermic peak in 200–300°C represents the carbon deposition on the metal surface, as metal can catalyse the coke combustion process in a certain degree. The exothermic peaks within 380–500 and 500–630°C are for the carbon and the graphitised carbon on support [24], respectively. According to the DTA curve, the second peak area of $\text{Pt}_3\text{Sn}/\text{Al}_2\text{O}_3$ accounts for the most proportion, indicating the most carbon deposits after reaction are on the support. Therefore, the majority of Pt_3Sn alloy exposed on the catalyst after carbon deposit can maintain high stability in propane dehydrogenation. According to the weight loss curve of the catalyst after the reaction, the content of carbon deposit was calculated to be 5.3% (from 200 to 800°C). Dehydrogenation is a structure-insensitive reaction, meaning that very small Pt or Pt–Sn clusters are preferred. However, undesired side reactions such as coke formation are sensitive to the structure of the Pt particles and require relatively large ensembles of Pt. Pt–Sn nanoalloy catalyst has a small particle size and effectively curb the structure-sensitive reactions. Additionally, it is also favourable for the migration of coke precursors from the Pt–Sn surface to the support, effectively reducing the effects of coke deposition [13, 25].

4. Conclusion: In summary, a new Pt–Sn/ Al_2O_3 nanoalloy catalyst was prepared through a carbonylation–impregnation method. The bimetallic Pt_xSn_y carbonyl cluster compounds were synthesised and used as a precursor for the achievement of small Pt–Sn bimetallic catalyst. In the impregnation process, this allows approaching the precise control over composition in the active centre on the surface of Al_2O_3 support instead of random anchoring of Pt or Sn components. The N_2 adsorption–desorption isotherm test shows the material has a mesoporous channel, with pore size distributed within 5–8 nm. The structural characterisations demonstrate the existence of Pt_3Sn alloy with exposing (111) and (200) facets. In the propane dehydrogenation, the as-prepared Pt–Sn/ Al_2O_3 catalyst exhibits good propane dehydrogenation performance and stability. After the reaction proceeds for 12 h, a propane conversion of 27.1% and a propylene selectivity of 93.3% were achieved. The carbon deposit of catalyst mainly existed on the support surface.

5. Acknowledgments: The authors are grateful to the financial supports of the National Natural Science Foundation of China

(grant no. 21506255) and the Promotive Research Fund for Excellent Young and Middle-aged Scientists of Shandong Province (grant no. BS2014NJ010) and the Shandong Provincial Natural Science Foundation (grant no. ZR2016BM12).

6 References

- [1] Li B., Xu Z.X., Jing F.L., *ET AL.*: 'Facile one-pot synthesized ordered mesoporous Mg-SBA-15 supported PtSn catalysts for propane dehydrogenation', *Appl. Catal. A, Gen.*, 2017, **533**, pp. 17–27
- [2] Sun C., Lou J., Cao M., *ET AL.*: 'A comparative study on different regeneration processes of Pt–Sn/ γ - Al_2O_3 catalysts for propane dehydrogenation', *J. Energy Chem.*, 2018, **27**, pp. 311–318
- [3] Prakash N., Lee M.H., Yoon S.H., *ET AL.*: 'Role of acid solvent to prepare highly active PtSn/ θ - Al_2O_3 catalysts in dehydrogenation of propane to propylene', *Catal. Today*, 2017, **293–294**, pp. 33–41
- [4] Ricca A., Palma V., Iaquaniello G., *ET AL.*: 'Highly selective propylene production in a membrane assisted catalytic propane dehydrogenation', *Chem. Eng. J.*, 2017, **330**, pp. 1119–1127
- [5] Sattler J.J., Ruiz-Martinez J., Santillan-Jimenez E., *ET AL.*: 'Catalytic dehydrogenation of light alkanes on metals and metal oxides', *Chem. Rev.*, 2014, **114**, pp. 10613–10653
- [6] Kaylor N., Davis R.J.: 'Propane dehydrogenation over supported Pt–Sn nanoparticles', *J. Catal.*, 2018, **367**, pp. 181–193
- [7] James O.O., Mandal S., Alele N., *ET AL.*: 'Lower alkanes dehydrogenation: strategies and reaction routes to corresponding alkenes', *Fuel Process. Technol.*, 2016, **149**, pp. 239–255
- [8] Shan Y.L., Sui Z.J., Zhu Y., *ET AL.*: 'Effect of steam addition on the structure and activity of Pt–Sn catalysts in propane dehydrogenation', *Chem. Eng. J.*, 2015, **278**, pp. 240–248
- [9] Kumar M.S., Chen D., Holmen A., *ET AL.*: 'Dehydrogenation of propane over Pt-SBA-15 and Pt–Sn-SBA-15: effect of Sn on the dispersion of Pt and catalytic behavior', *Catal. Today*, 2009, **142**, pp. 17–23
- [10] Iglesias-Juez A., Beale A.M., Maaijen K., *ET AL.*: 'A combined in situ time-resolved UV-Vis, Raman and high-energy resolution X-ray absorption spectroscopy study on the deactivation behavior of Pt and Pt–Sn propane dehydrogenation catalysts under industrial reaction conditions', *J. Catal.*, 2010, **276**, pp. 268–279
- [11] Kappenstein C., Guérin M., Lázár K., *ET AL.*: 'Characterisation and activity in *n*-hexane rearrangement reactions of metallic phases on catalysts of Pt–Sn/ Al_2O_3 different preparations', *J. Chem. Soc., Faraday Trans.*, 1998, **94**, pp. 2463–2473
- [12] Vu B.K., Song M.B., Ahn I.Y., *ET AL.*: 'Pt–Sn alloy phases and coke mobility over Pt–Sn/ Al_2O_3 and Pt–Sn/ ZnAl_2O_4 catalysts for propane dehydrogenation', *Appl. Catal. A, Gen.*, 2011, **400**, pp. 25–33
- [13] Yang M.L., Zhu Y., Zhou X.G., *ET AL.*: 'First-principles calculations of propane dehydrogenation over PtSn catalysts', *ACS Catal.*, 2012, **2**, pp. 1247–1258
- [14] Dautzenberg F.M., Helle J.N., Biloen P., *ET AL.*: 'Conversion of *n*-hexane over monofunctional supported and unsupported PtSn catalysts', *J. Catal.*, 1980, **63**, pp. 119–128
- [15] Dickinson A.J., Carrette L.P.L., Collins J.A., *ET AL.*: 'Preparation of a Pt–Ru/C catalyst from carbonyl complexes for fuel cell applications', *Electrochim. Acta*, 2002, **47**, pp. 3733–3739
- [16] Shitova N.B., Perfil'ev Y.D., Al't L.Y., *ET AL.*: 'Reaction of polynuclear platinum carbonyl with tin(II) chloride', *Russ. J. Inorg. Chem.*, 2001, **46**, pp. 376–381
- [17] Johnson B.F.G., Raynor S.A., Brown D.B., *ET AL.*: 'New catalysts for clean technology', *J. Mol. Catal. A, Chem.*, 2002, **182–183**, pp. 89–97
- [18] Liu J., Liu C.C., Ma A.Z., *ET AL.*: 'Effects of Al_2O_3 phase and Cl component on dehydrogenation of propane', *Appl. Surf. Sci.*, 2016, **368**, pp. 233–240
- [19] Zhang Y.W., Zhou Y.M., Shi J.J., *ET AL.*: 'Comparative study of bimetallic Pt–Sn catalysts supported on different supports for propane dehydrogenation', *J. Mol. Catal. A, Chem.*, 2014, **381**, pp. 138–147
- [20] Liu X., Lang W.Z., Long L.L., *ET AL.*: 'Improved catalytic performance in propane dehydrogenation of PtSn/ γ - Al_2O_3 catalysts by doping indium', *Chem. Eng. J.*, 2014, **247**, pp. 183–192
- [21] Zhou H.L., Gong J.J., Xu B.L., *ET AL.*: 'PtSnNa/SUZ-4: an efficient catalyst for propane dehydrogenation', *Chin. J. Catal.*, 2017, **38**, pp. 529–536

- [22] Li Q.: 'The kinetics of propane dehydrogenation and coke formation over Pt catalysts'. PhD thesis, East China University of Science and Technology, 2012
- [23] Sokolov S., Stoyanova M., Rodemerck U., *ET AL.*: 'Comparative study of propane dehydrogenation over V-, Cr-, and Pt-based catalysts: time on-stream behavior and origins of deactivation', *J. Catal.*, 2012, **293**, pp. 67–75
- [24] Larsson M., Hultén M., Blekkan E.A., *ET AL.*: 'The effect of reaction conditions and time on stream on the coke formed during propane dehydrogenation', *J. Catal.*, 1996, **164**, pp. 44–53
- [25] Yu C.L., Xu H.Y., Ge Q.J., *ET AL.*: 'Properties of the metallic phase of zinc-doped platinum catalysts for propane dehydrogenation', *J. Mol. Catal. A, Chem.*, 2007, **266**, pp. 80–87